ADVANCES IN ATMOSPHERIC SCIENCES, VOL. 28, NO. 6, 2011, 1266–1278

Response of a Grassland Ecosystem to Climate Change in a Theoretical Model

SUN Guodong*[1] (孙国栋) and MU Mu[2,1] (穆 穆)

[1] *The State Key Laboratory of Numerical Modeling for Atmospheric Sciences and Geophysical Fluid Dynamics, Institute of Atmospheric Physics, Chinese Academy of Sciences, Beijing* 100029

[2] *Key Laboratory of Ocean Circulation and Wave, Institute of Oceanology, Chinese Academy of Sciences, Qingdao* 266071

(Received 15 November 2010; revised 1 February 2011)

ABSTRACT

The response of a grassland ecosystem to climate change is discussed within the context of a theoretical model. An optimization approach, a conditional nonlinear optimal perturbation related to parameter (CNOP-P) approach, was employed in this study. The CNOP-P, a perturbation of moisture index in the theoretical model, represents a nonlinear climate perturbation. Two kinds of linear climate perturbations were also used to study the response of the grassland ecosystem to different types of climate changes.

The results show that the extent of grassland ecosystem variation caused by the CNOP-P-type climate change is greater than that caused by the two linear types of climate change. In addition, the grassland ecosystem affected by the CNOP-P-type climate change evolved into a desert ecosystem, and the two linear types of climate changes failed within a specific amplitude range when the moisture index recovered to its reference state. Therefore, the grassland ecosystem response to climate change was nonlinear. This study yielded similar results for a desert ecosystem seeded with both living and wilted biomass litter. The quantitative analysis performed in this study also accounted for the role of soil moisture in the root zone and the shading effect of wilted biomass on the grassland ecosystem through nonlinear interactions between soil and vegetation. The results of this study imply that the CNOP-P approach is a potentially effective tool for assessing the impact of nonlinear climate change on grassland ecosystems.

Key words: conditional nonlinear optimal perturbation, parameter perturbation, CNOP-P, grassland ecosystem, climate change

Citation: Sun, G. D., and M. Mu, 2011: Response of a grassland ecosystem to climate change in a theoretical model. *Adv. Atmos. Sci.*, **28**(6), 1266–1278, doi: 10.1007/s00376-011-0169-6.

1. Introduction

The degeneration of grassland ecosystems has been the focus of much research in recent decades. Observational and numerical modeling studies have indicated that temporal and spatial degeneration often occurs due to climate change and human activity (Woodward, 1987; Klausmeier, 1999; Zeng et al., 2002; Ni, 2004; Woodward et al., 2004; Notaro et al., 2006; Liu et al., 2006a). Such degeneration can have a great impact on climate conditions and the terrestrial carbon cycle (Xue and Shukla, 1993; Xue, 1996; Gao et al., 2003; Piao et al., 2007; Jia et al., 2007). Therefore, it is important to investigate the potential responses of grassland ecosystems to climate change.

Climate change has an important influence on grassland ecosystems, and many studies have investigated the response of these systems to such changes. For example, Claussen et al. (1999) demonstrated that the positive interaction between vegetation and climate was an important desertification mechanism within a complex model in the Sahel. Within a simple model, one possible mechanism for desertification was associated with climate variability (Liu et al., 2006b). Zeng and Neelin (2000) emphasized that climate variability could smooth the gradient from desert to forest

*Corresponding author: SUN Guodong, sungd@mail.iap.ac.cn

in the African savanna region due to the nonlinearity of coupled ecosystems, which favored the maintenance of unstable and grassland-like states. These investigations generally concerned climate change relative to desertification mechanisms. However, whether simple or complex models were used, there has been little discussion of the response of grassland ecosystems to nonlinear climate change or of the potential use of a nonlinear optimization method to analyze differences in grassland responses to nonlinear and linear climate changes. Recently, Mu and Wang (2007) employed a nonlinear optimization method involving a conditional nonlinear optimal perturbation related to the initial condition (CNOP-I, Mu et al., 2003) and the linear singular vector (LSV) to identify nonlinear stability in the grassland ecosystems of Inner Mongolia. Their results prompted this study of the response of grassland ecosystems to nonlinear climate change using a nonlinear optimization method.

A conditional nonlinear optimal perturbation related to parameter (CNOP-P) approach (Mu et al., 2010), based on the conditional nonlinear optimal perturbation related to initial perturbations (CNOP-I) approach (Mu et al., 2003), is a nonlinear optimization method. The CNOP-I approach has been used to investigate the dynamics of ENSO predictability, prediction error (Mu and Duan, 2003; Duan et al., 2004; Duan and Mu, 2006; Mu et al., 2007a), the nonlinear stability of steady states of thermohaline circulation (Mu et al., 2004; Sun et al., 2005), ensemble prediction (Mu and Jiang, 2008), adaptive observation (Mu et al., 2007b) and grassland ecosystems (Mu and Wang, 2007; Sun and Mu, 2009). These applications illustrate that the CNOP approach is a useful tool for studying nonlinear systems.

In this study, we explored the response of grassland ecosystems to nonlinear climate change, both to assess differences between the responses of grassland ecosystems to nonlinear and linear climate changes using a five-variable theoretical grassland ecosystem model (Zeng et al., 2006) in Inner Mongolia, and to determine how the impacted grassland (desert) ecosystem reacts when the climate condition reverts to the reference state. The CNOP-P, which represents the perturbation of the moisture index in the theoretical model, can be regarded as the most nonlinearly unstable (or most sensitive) climatic perturbation.

2. The model and method

2.1 *The five-variable grassland ecosystem model*

A simple theoretical model is an appropriate method to investigate the response of the grassland ecosystem to climate change. In the section, the five-variable grassland ecosystem model is introduced.

The five-variable grassland ecosystem model includes a three-variable ecosystem model and a three-layer land-surface hydrological model dealing with one species of grass (Zeng et al., 2005) native to Inner Mongolia. The model uses the following equations:

$$
\begin{aligned}
\frac{dM_{\rm c}}{dt} =& \alpha^*[G(M_{\rm c},W_{\rm r}) - D_{\rm c}(M_{\rm c},W_{\rm r}) - C_{\rm c}(M_{\rm c})] \,, \\
\frac{dM_{\rm d}}{dt} =& \alpha^*[\beta^{'} D_{\rm c}(M_{\rm c},W_{\rm r}) - D_{\rm d}(M_{\rm d}) - C_{\rm d}(M_{\rm d})] \,, \\
\frac{dW_{\rm c}}{dt} =& P_{\rm c}(M_{\rm c}) + E_{\rm r}(M_{\rm c},W_{\rm r}) - \\
& E_{\rm c}(M_{\rm c},W_{\rm r}) - R_{\rm c}(M_{\rm c}) \,, \\
\frac{dW_{\rm s}}{dt} =& P_{\rm s}(M_{\rm c}) - E_{\rm s}(M_{\rm c},W_{\rm s},M_{\rm d}) + R_{\rm c}(M_{\rm c}) - \\
& Q_{\rm sr}(W_{\rm s},W_{\rm r}) - R_{\rm s}(M_{\rm c},W_{\rm s},M_{\rm d}) \,, \\
\frac{dW_{\rm r}}{dt} =& P_{\rm r}(M_{\rm c}) + \alpha_{\rm r} R_{\rm s}(M_{\rm c},W_{\rm s},M_{\rm d}) - \\
& E_{\rm r}(M_{\rm c},W_{\rm r}) + Q_{\rm sr}(W_{\rm s},W_{\rm r}) - R_{\rm r}(M_{\rm c},W_{\rm r}) \,.
\end{aligned}
$$

where the variables of the model are living biomass ($M_{\rm c}$), wilted biomass ($M_{\rm d}$), water content in the vegetation canopy ($W_{\rm c}$), water content in the thin surface layer of soil ($W_{\rm s}$) and water content in the rooting layer ($W_{\rm r}$). More details about the model parameters and their physical explanations can be found in the appendix. Although the model is simple, it clearly and concisely represents the essential features of the complex atmosphere-ecosystem-soil system, including multiple equilibria, bifurcation and abrupt changes. This model has also been employed to investigate the nonlinear stability of the grassland equilibrium in response to human activity (Sun and Mu, 2009).

2.2 *Conditional nonlinear optimal perturbation: Parameter perturbation*

To study the first kind of predictability, Mu et al. (2003) proposed the CNOP-I approach. As the nonlinear generalization of the linear singular vector, the CNOP-I is the initial perturbation whose nonlinear evolution attains the maximal value of a cost function at a given time subject to the constraint conditions. In the work of Mu et al. (2010), the CNOP-P approach was proposed for studying the second kind of predictability. The CNOP-P is the parameter perturbation whose nonlinear evolution attains the maximal value of a cost function. Here, we review the derivation of this approach. The nonlinear differential equations

follow:

$$\begin{cases} \dfrac{\partial \boldsymbol{U}}{\partial t} = F(\boldsymbol{U},\ \boldsymbol{P}(t)) & \boldsymbol{U} \in R^n, t \in [0, t'] \\ \boldsymbol{U}|_{\mathrm{t}=0} = \boldsymbol{U}_0 \\ \boldsymbol{P}|_{\mathrm{t}=0} = \boldsymbol{P}_0 \end{cases} \tag{1}$$

where F is a nonlinear continuous operator, $\boldsymbol{U}_0$ is an initial value, and $\boldsymbol{P}(t)$ is a time-dependent parameter vector. R^n is the n-dimensional vector space.

Let M_τ be the propagator of the nonlinear differential equations from the initial time 0 to τ, and let $\boldsymbol{U}(\tau; \boldsymbol{U}_0, \boldsymbol{P}(t))$ be a solution of the nonlinear equations at time τ, and satisfies $\boldsymbol{U}(\tau; \boldsymbol{U}_0, \boldsymbol{P}(t)) = M_\tau(\boldsymbol{U}_0, \boldsymbol{P}(t))$, and $\boldsymbol{P}(t)$ indicates time-dependent from the initial time 0 to τ during the integration of the model.

Let $\boldsymbol{U}(t'; \boldsymbol{U}_0, \boldsymbol{P}(t))$ and $\boldsymbol{U}(t'; \boldsymbol{U}_0, \boldsymbol{P}(t)) + \boldsymbol{u}(t'; \boldsymbol{U}_0, \boldsymbol{p}(t))$ be the solutions of the nonlinear differential Eq. (1), with parameters vector $\boldsymbol{P}(t)$ and $\boldsymbol{P}(t) + \boldsymbol{p}(t)$ respectively, where $\boldsymbol{p}(t)$ is a parameter perturbation and $\boldsymbol{U}_0$ is an initial value. The solutions satisfy

$$\begin{cases} \boldsymbol{U}(t'; \boldsymbol{U}_0, \boldsymbol{P}(t)) = M_{\mathrm{t}'}(\boldsymbol{U}_0, \boldsymbol{P}(t)) \ , \\ \boldsymbol{U}(t'; \boldsymbol{U}_0, \boldsymbol{P}(t)) + \boldsymbol{u}(t'; \boldsymbol{U}_0, \boldsymbol{p}(t)) = M_{\mathrm{t}'}(\boldsymbol{U}_0, \boldsymbol{P}(t) + \boldsymbol{p}(t)) \ . \end{cases}$$

For a proper norm $\|\cdot\|$, a parameter perturbation $\boldsymbol{p}_\delta(t)$ is called a CNOP-P if and only if

$$J(\boldsymbol{p}_\delta(t)) = \max_{\boldsymbol{p}(t)\in\Omega} J(\boldsymbol{p}(t)) \ , \tag{2}$$

where

$$J(\boldsymbol{p}(t)) = \|M_{\mathrm{t}'}(\boldsymbol{U}_0, \boldsymbol{P}(t) + \boldsymbol{p}(t)) - M_{\mathrm{t}'}(\boldsymbol{U}_0, \boldsymbol{P}(t))\| \ . \tag{3}$$

$\boldsymbol{P}(t)$ is a reference state, $\boldsymbol{p}(t)$ is the perturbation of the reference state, and $\boldsymbol{p}(t) \in \Omega$ is a constraint condition. In general, the constraint condition is $\|\boldsymbol{p}(t)\| \leqslant \delta$, and δ is the constraint condition parameter and represents the amplitude of the parameter perturbation that the CNOP-P is the parameter perturbation whose nonlinear evolution attains the maximum value of the cost function J at time t'.

To obtain the maximum value of Eq. (2), the sequential quadratic programming (SQP) algorithm (Barclay et al., 1997) was employed. Mu et al. (2003) reported the details regarding this algorithm. The gradients of the cost function were computed using the definition of the gradient.

2.3 *Experimental design*

An important parameter in the five-variable grassland ecosystem model is the moisture index μ, expressed as the ratio of annual precipitation to annual potential evaporation. Although some studies have examined the impact of interaction between parameters on the Earth system (Hallgren and Pitman, 2000; Rosero et al., 2010), the moisture index as a parameter was applied to explore the response of grasslands to climate change in this study. Because this ratio represents a climatic condition, it was appropriate to examine the response of the grassland ecosystem to climate change using this parameter. In our experiment, the moisture index μ was regarded as an optimization parameter, and its reference state was constant during the optimization time. Two moisture indices (μ=0.305 and μ=0.31) and two optimization times (t'=15 years and t'=20 years) were considered in order to determine whether or not the numerical results are dependent on the reference state and the optimization time. The model was discretized based on the fourth-order Runge-Kutta method with a time step of $dt = 1/24$ (representing half a month). In Eq. (3), $\boldsymbol{P}(t)$ and $\boldsymbol{p}(t)$ are continuous but are actually be discretized according to the optimization time.

To analyze the grassland ecosystem response to climate change, we ran the model with the ecosystem equilibrium state at the initial value for the CNOP-P-type climate change during the optimization time. Afterward, the model was run successively with the reference state of the moisture index, to depict variations in the grassland ecosystem. If the grassland ecosystem degenerated into a desert ecosystem, it became unstable and underwent an abrupt change; otherwise, the grassland ecosystem was stable. Two kinds of linear parameter perturbations were designed to investigate the nonlinear character of the response. Although the parameter perturbation types were disparate, their amplitudes were uniform.

3. Numerical results

3.1 *Response of the grassland ecosystem to the CNOP-P-type climate change*

In this section, the moisture index μ was set at 0.31 as the reference state, and the numerical results are presented for the optimization time t'=20 years.

Two different equilibrium states were chosen. First, the linearly stable grassland equilibrium state A was chosen, where $x = 0.553$ represents the living

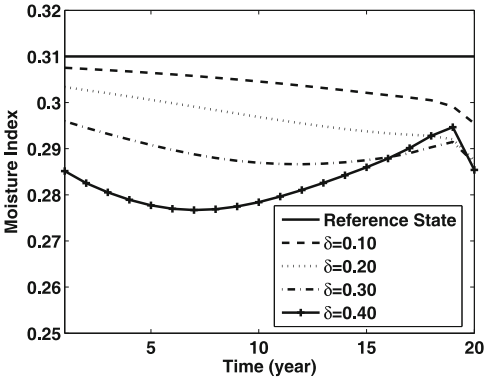

Fig. 1. Annual variation of moisture indices caused by the CNOP-Ps superimposed upon the reference state (μ=0.31) for the different constraint conditions for the grassland ecosystem, with an optimization time of 20 years (t'=20 yr).

biomass, $y_1 = 0.641$ represents the water content in the thin soil surface layer, $y_2 = 0.653$ represents the water content in the rooting layer, and $z = 0.580$ represents the wilted biomass. Second, the linearly stable desert equilibrium state B was chosen, where $x = 0.000, y_1 = 0.368, y_2 = 0.415$, and $z = 0.000$. For the desert equilibrium state, the response to climate change was minor because there was no living biomass, but this lack of living biomass was not taken into account. Therefore, for the desert equilibrium state, living and wilted biomass terms were set to 0.1, which represents $\sim$0.01 kg m^{-2}.

Figure 1 shows the annual variation in the moisture index μ during the optimization time, where the CNOP-P was superimposed on the reference state. For the different constraint condition parameters, the variations in moisture index were nonlinear. When the CNOP-P was superimposed upon the reference state, the moisture index lessened during the optimization time. The parameter perturbation that caused the grassland equilibrium state to become the least stable resulted in severe drought. Furthermore, the patterns of moisture indices were distinct for the different constraint conditions. For the small constraint condition parameter (δ=0.1 and δ=0.2), the moisture index resulting from the CNOP-P gradually decreased. When the constraint condition parameter was enhanced (δ=0.3 and δ=0.4), the moisture index from the CNOP-P gradually decreased in the initial phase,

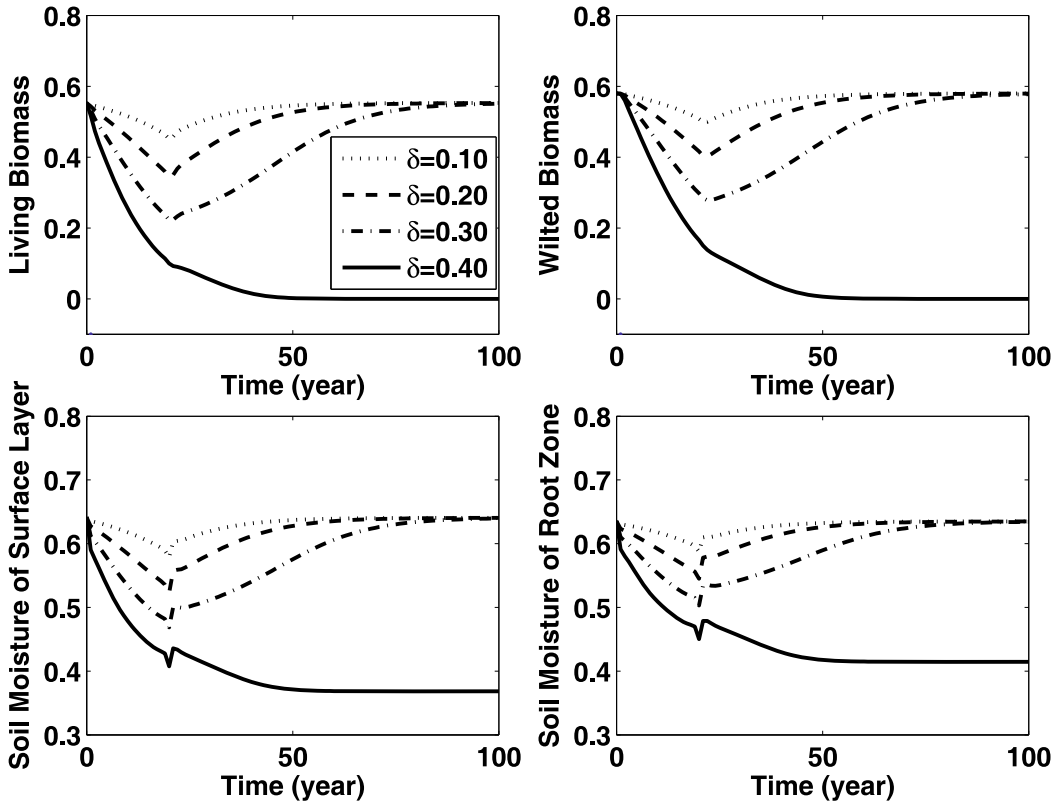

Fig. 2. The nonlinear evolution of four components of the grassland ecosystem influenced by CNOP-P-type climate change and their evolution when the moisture index recovered to the reference state.

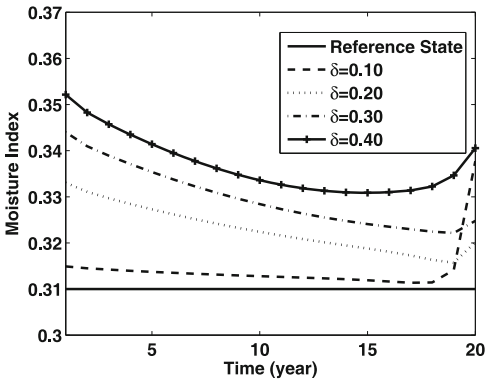

Fig. 3. Same as Fig. 1, but for the desert ecosystem.

increased in the following years, and ultimately decreased rapidly.

We also analyzed the grassland equilibrium state response to CNOP-P-type climate change in the first 20 years. We also analyzed how the altered grassland ecosystem recovered when the moisture index returned to the reference state. The nonlinear evolution for the different constraint conditions of four components in grassland ecosystems are presented in Fig. 2. The four components decreased during the optimization time due to the lower moisture index. Great dissimilarity occurred among the different constraint conditions in the nonlinear evolution of the four components when the moisture index was equal to the reference state. In the cases of δ=0.1, δ=0.2, or δ=0.3, the grassland ecosystem, influenced by the CNOP-P-type climate change, recovered to the grassland equilibrium state; the difference lay in the time required for recovery. However, for δ=0.4, the grassland ecosystem evolved into a desert equilibrium state, and the abrupt change occurred. The numerical results indicate that, when it is influenced by a sufficiently large climate change, the grassland ecosystem evolves to the desert state even when the moisture index returns to the reference state.

For the desert ecosystem, the CNOP-Ps were obtained for different constraint conditions with the optimization time of 20 years. The temporal patterns of the moisture indices, which were the CNOP-Ps superimposed upon the reference state for the four constraint conditions, are shown in Fig. 3. All four constraint conditions show that the moisture indices initially increased, decreased in the first phase, and increased again in the later years of the optimization time. This trend illustrates how the parameter perturbation, which led to the most unstable desert equilibrium state, produced high moisture in this climatic condition.

This study demonstrates how the desert ecosystem responds to the CNOP-P-type climate change in the

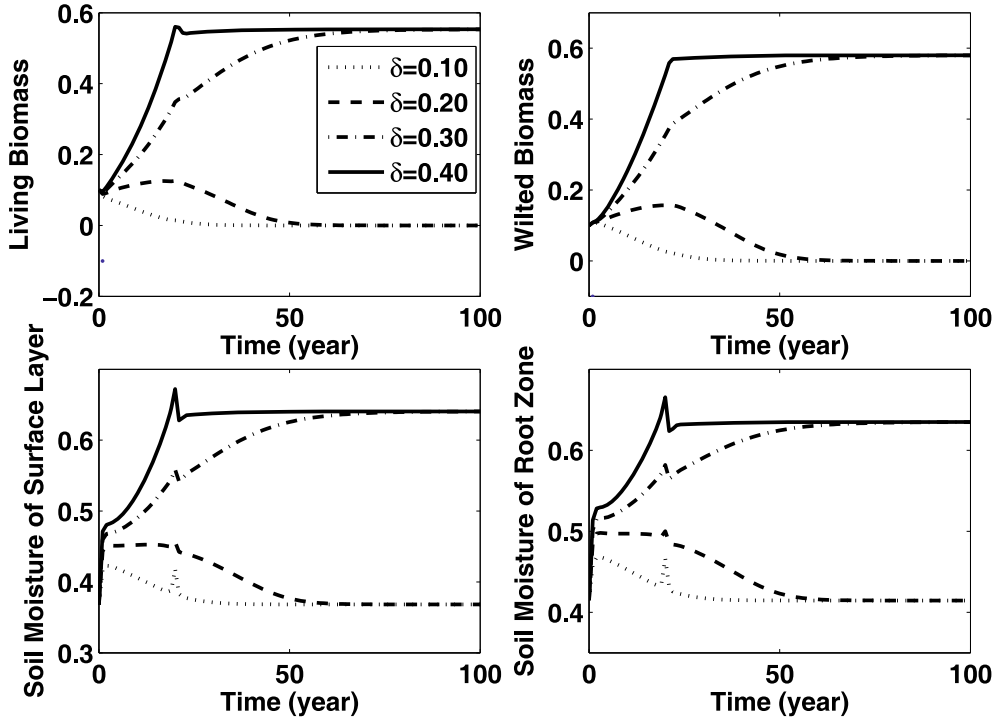

Fig. 4. Same as Fig. 2, but for the desert ecosystem.

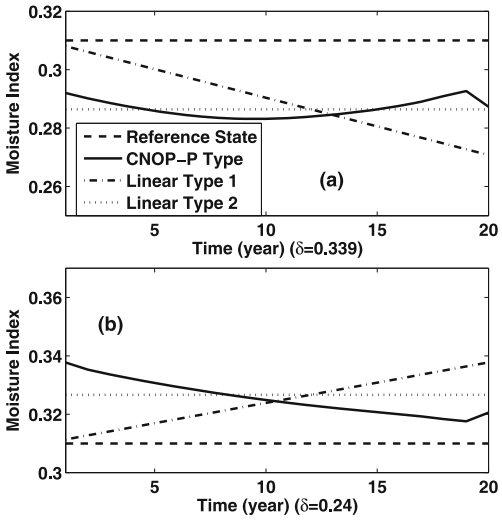

Fig. 5. The annual variation in moisture indices for the different types of climate change: (a) the grassland ecosystem; (b) the desert ecosystem.

first 20 years and how the ecosystem is influenced by climate change when the moisture index reverts to the reference state. Figure 4 shows that the four components of the desert ecosystem were enhanced during the optimization time. When influenced by the CNOP-P-type climate change with the moisture index at the reference state, the desert ecosystem will recover to the desert equilibrium state when δ=0.1 or δ=0.2, the only difference lies in the recovery time. Simply put, the larger the constraint condition parameter, the longer the recovery time. In the case of δ=0.3 or δ=0.4, the desert ecosystem influenced by the CNOP-P-type climate change will attain the grassland equilibrium state. The numerical results show that a desert ecosystem, influenced by a sufficiently large CNOP-P-type climate change and provided with a litter of living biomass and wilted biomass, is nonlinearly unstable.

3.2 *Comparison of responses to nonlinear climate change and linear climate change*

As shown above, the moisture indices caused by the CNOP-Ps had nonlinear character. How was the nonlinear evolution of the grassland ecosystem influenced by nonlinear or linear climate change? To illustrate the discrepancy between the two, we designed two linear climate perturbations that could be classified by their line slope, which was either zero or nonzero. Figure 5 shows the temporal variation around the moisture indices for the different parameters. The amplitudes of the parameter perturbations were δ=0.339 for the grassland ecosystem and δ=0.24 for the desert ecosystem.

For the grassland equilibrium state, the responses to different types of climate change for the same optimization time and the same amplitude of parameter perturbation are presented. For δ=0.1, δ=0.2, δ=0.3, or δ=0.4, the variability of the grassland ecosystem influenced by the CNOP-P-type climate change was larger than what would be seen in the two linear climate change types for a given optimization time (Table 1). This implies that nonlinear climate change had a severe impact on the grassland ecosystem; as δ, increased, the phenomenon became more visible. Figure 6a shows the nonlinear evolution of the grassland ecosystem as influenced by CNOP-P-type climate change and two types of linear climate change for δ=0.339. For convenience, the living biomass of the grassland equilibrium state A was also plotted. During the optimization time, living biomass gradually decreased due to climate change in the first 20 years. When the moisture index returned to the reference state, the grassland ecosystem influenced by the CNOP-P-type climate change, degenerated into the desert equilibrium state and became nonlinearly unstable. However, grassland ecosystems influenced by one of the two types of linear climate changes fail. These results are similar to those of Mitchell and Csillag (2001) when the applied the Century model. The numerical results show that the response of the grassland ecosystem to climate change is nonlinear.

The response to climate change was nonlinear for the desert ecosystem as well. For the given optimization time, the variability of the desert ecosystem influenced by the CNOP-P-type climate change and provided with a litter of living and wilted biomass was larger than the variability found for the two types of linear climate change (Table 2). Figure 6b shows that the desert ecosystem influenced by the CNOP-P-type

Table 1. The relative change of the grassland ecosystem caused by three types of climate change for t'=20 yr.

δ	CNOP-P Type	Linear Type 1	Linear Type 2
0.1	0.121	0.120	0.111
0.2	0.252	0.249	0.243
0.3	0.402	0.379	0.399
0.4	0.566	0.504	0.557

Table 2. Same as Table 1, but for the desert ecosystem.

δ	CNOP-P Type	Linear Type 1	Linear Type 2
0.1	0.141	0.106	0.126
0.2	0.425	0.219	0.368
0.3	1.005	0.423	0.896
0.4	1.556	0.769	1.491

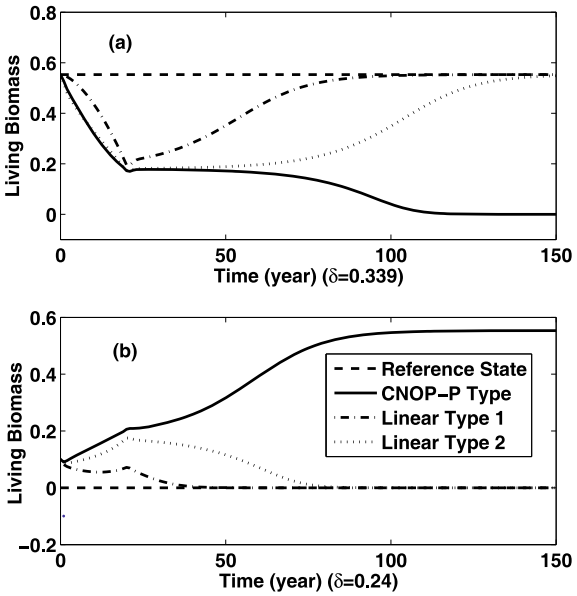

Fig. 6. The nonlinear evolution of the living biomass influenced by different climate change types and their evolution when the moisture index recovers to the reference state: (a) the grassland ecosystem; (b) the desert ecosystem.

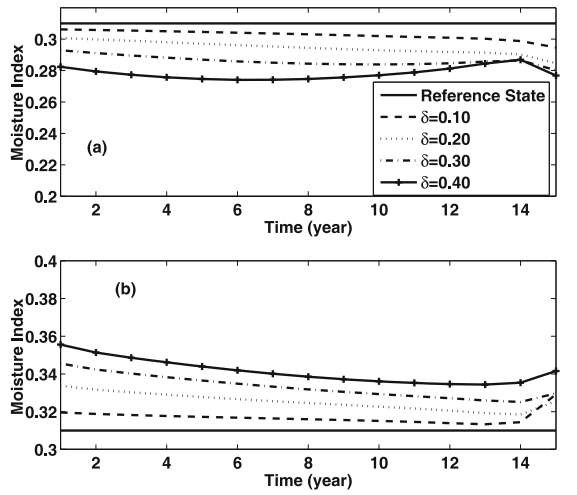

Fig. 7. Same as Figs. 1 and 3, but for the optimization time of 15 years and the reference state μ=0.31: (a) the grassland ecosystem; (b) the desert ecosystem.

climate change evolved into the grassland equilibrium state when the moisture index recovered to the reference state. However, the desert ecosystems that were influenced by the two kinds of linear climate change failed.

3.3 *The interaction between the vegetation and the soil*

In recent research, there is much discussion about the mechanism of grassland degeneration (Zeng and Neelin, 2000; Liu et al., 2006b). In the present study, we analyzed the variation of the grassland ecosystem as a consequence of the interaction between the vegetation and the soil (Zeng et al., 2005).

Within this five-variable grassland ecosystem model, the maintenance and the degradation of the grassland directly depend on the variation of living biomass and on the variation of the soil moisture within the root zone. The gain (deficit) in living biomass needs a certain amount of soil moisture in the root zone in order to satisfy the its annual variation $\triangle x > 0$ ($\triangle x < 0$). During the first 20 years, the four components of the grassland ecosystem decreased due to the reduction of moisture indices. When the moisture index recovered to the reference state, the effects were complex. Because the soil moisture in the root zone affected by the CNOP-P-type climate change did not reach a certain threshold when δ=0.4 and t'=20 yr, the annual variation of the living biomass $\triangle x < 0$ and the annual variation of the wilted biomass $\triangle z < 0$. It follows that in the year 21, the living biomass and the wilted biomass both decreased. The variations $\triangle y_1$ and $\triangle y_2$, i.e., the soil moisture in the surface layer and root zone, were positive. Although the soil moisture increased, this did not ensure that variation in living and wilted biomass were positive. Because of this persistent reduction in living and wilted biomass, the shading effect of the wilted biomass weakened, and evaporation (E_s) and runoff (R_s) of the surface layer were enhanced. In year 22, the soil moisture of the surface layer decreased, and in year 23, the soil moisture in the root zone decreased while the runoff of the root zone (R_r) increased. The interaction between the vegetation and the soil moisture was responsible for this abrupt shift. When δ=0.1, δ=0.2, or δ=0.3, the soil moisture in the root zone did not decrease beyond a certain amount, and the variation in living biomass influenced by CNOP-P-type climate change was positive. Therefore, the transition from the grassland ecosystem to the desert ecosystem failed.

Different types of climate change lead to different levels of variation in grassland ecosystems. The primary difference lies in whether the soil moisture in the root zone decreases past a certain level. When δ=0.339, the soil moisture in the root zone influenced by the CNOP-P-type climate change decreased to a particular threshold, and the amounts of living and wilted biomass decreased. The persistent decrease in wilted biomass led to a weakening of the shading effect,

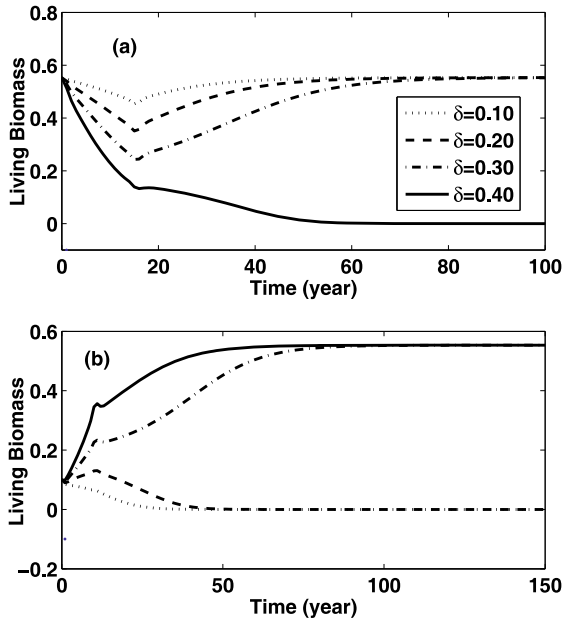

Fig. 8. The nonlinear evolution of living biomass influenced by CNOP-P-type climate change and their evolution when the moisture index recovered to the reference state for the optimization time of 15 years: (a) the grassland ecosystem; (b) the desert ecosystem.

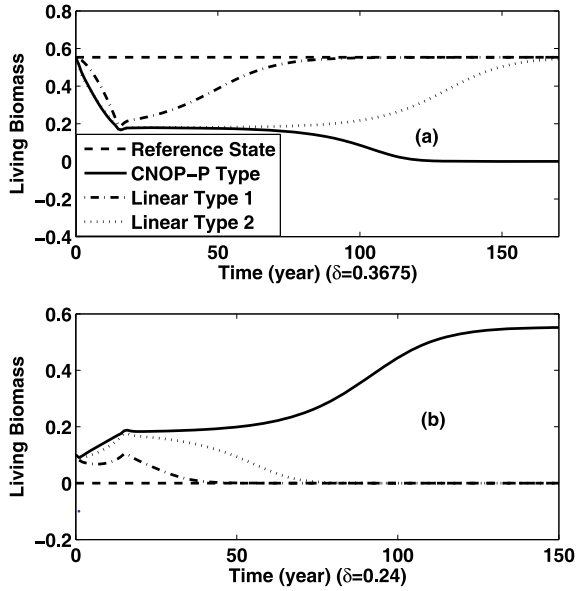

Fig. 9. Same as Fig. 6, but for the optimization time of 15 years: (a) the grassland ecosystem; (b) the desert ecosystem.

and evaporation (E_s) and runoff (R_s) intensified in turn. Eventually, the grassland ecosystem transitioned to a desert ecosystem. In contrast, because soil moisture in the root zone influenced by either of the two linear types of climate change did not decrease past this threshold, living biomass increased and no transition occurred. Our results show that the amount of soil moisture in the root zone and the shading effect of wilted biomass are important for maintaining the grassland ecosystem. These results also validate the conclusions of Zeng et al. (2004), Mu and Wang (2007), and Sun and Mu (2009) about the shading effect of wilted biomass.

3.4 *Altering optimization time*

To assess the time-independence of the results described above, we briefly describe the effects of an optimization time of $t' = 15$ yr. The temporal variation in the moisture index caused by the CNOP-P over 15 years was similar to that over a 20-year period in the grassland and desert ecosystems (Fig. 7). The model design of the two linear parameter perturbation types for the 15-year period were analogous to those for the 20-year period.

Figure 8 shows that grassland and desert ecosystems influenced by a sufficiently large enough CNOP-P parameter perturbation were unstable when t'=15 yr. When δ=0.3675, the grassland ecosystem influenced by the CNOP-P-type climate change evolved into the desert equilibrium state. However, the grassland ecosystems that were influenced by either of the two linear climate-change types failed (Fig. 9a). For the desert ecosystem, the results were similar when δ=0.24 (Fig. 9b).

4. Altering reference state

To investigate the robustness of the numerical results, we evaluated the other reference state: μ=0.305. We selected a grassland equilibrium state where $x = 0.467, y_1 = 0.595, y_2 = 0.602$, and $z = 0.512$, and we selected a desert equilibrium state where $x = 0.000, y_1 = 0.361, y_2 = 0.407$, and $z = 0.000$. Importantly, the living and wilted biomass values for the desert ecosystem were 0.1 in both states.

The results of the temporal variation in the moisture index and the nonlinear evolution of grassland and desert ecosystems for the reference state μ=0.305 (Figs. 10 and 11) were similar to those for the reference state μ=0.31 (Figs. 7 and 8). For the same amplitude of parameter perturbation, the grassland (desert) ecosystem influenced by the CNOP-P-type climate change convert into the desert (grassland) equilibrium state, whereas those influenced by the two lin-

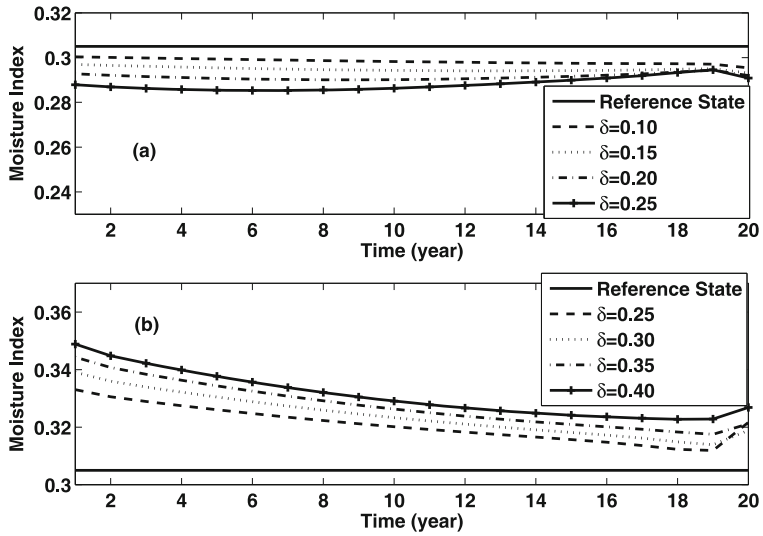

Fig. 10. Same as Fig. 7, but for the reference state μ=0.305: (a) the grassland ecosystem; (b) the desert ecosystem.

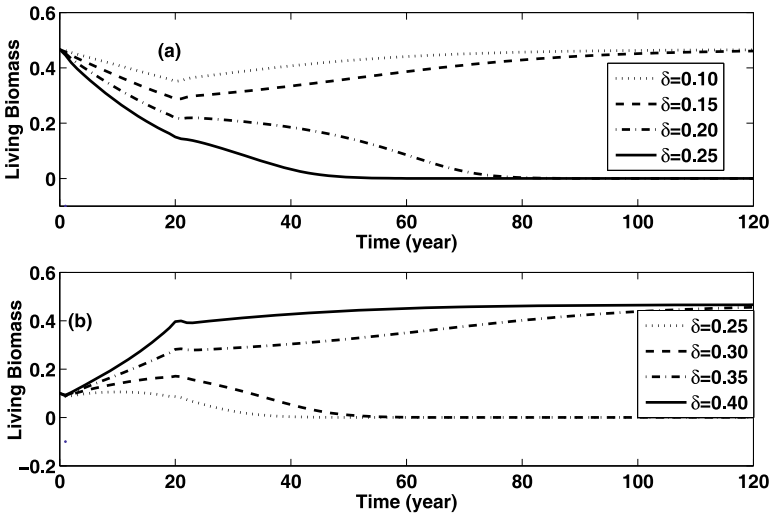

Fig. 11. Same as Fig. 8, but for the reference state μ=0.305: (a) the grassland ecosystem; (b) the desert ecosystem.

ear climate change types do not (Fig. 12).

5. Variations of the grassland ecosystem to real moisture index

To further explore the impact of nonlinear climate change on the grassland ecosystem, the moisture index derived from monthly precipitation and temperature data in Inner Mongolia was calculated. According to the definition of the moisture index $\mu = P_{\rm rec}/e_{\rm s}^*$, the precipitation and temperature data based on the data from 160 observational station obtained from the China Meteorological Administration were employed. $P_{\rm rec}$ and $e_{\rm s}^*$ denote the precipitation and the maximal potential evaporation from the soil surface layer. The maximal potential evaporation was calculated using (Ma and Fu, 2001):

$$e_{\rm s}^* = \begin{cases} 0 & (T \leqslant 0) \\ 1.6d(10T/I)^{\xi} & (0 \leqslant T \leqslant 26.5) \end{cases},$$

where T denotes monthly temperature, and d was

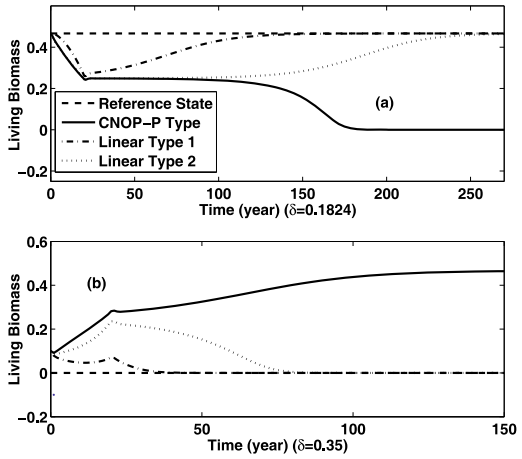

Fig. 12. Same as Fig. 9, but for the reference state μ=0.305: (a) the grassland ecosystem; (b) the desert ecosystem.

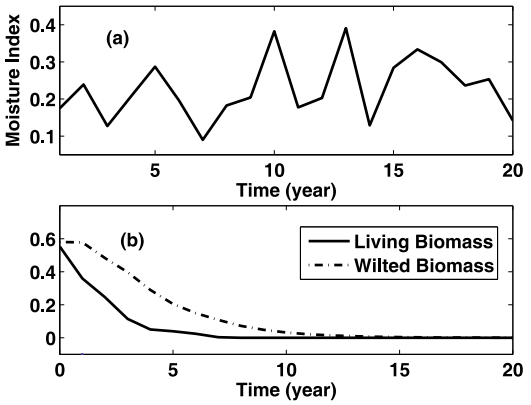

Fig. 13. The case of observational data: (a) the moisture index; (b) the nonlinear evolution of the grassland ecosystem.

equal to monthly number of days divided by 30. $\xi = 0.49239 + 1.792\times10^{-2}I - 7.71\times10^{-5}I^2 + 6.75\times10^{-7}I^3$, $I = \sum_{i=1}^{12}(\frac{T_i}{5})^{1.514}$. T_i represents the temperature in month i. The Urad Zhongqi (41.50°N, 108.28°E) was chosen based on the observed biomass amount and, of the 160 stations, the Shanba (40.58°N, 107.1°E) station is closest to Urad Zhongqi. The precipitation and temperature data from the Shanba station was applied over the period 1980–1999. The moisture index, which is similar to that calculated employing the CNOP-P approach, is given in Fig. 13a. The nonlinear evolution of the grassland ecosystem is shown in Fig. 13b. The change was abrupt when using the observational data, which might be due to the fact that biomass levels in the theoretical model decrease when climate conditions are poor. Our results are similar to the observational data on biomass levels in the Urad Zhongqi during the last 20 years of the 21st century (Ni, 2004).

6. Summary and discussion

Our objective was to investigate the nonlinear response of the grassland ecosystem to climate change using the CNOP-P approach. With sufficiently large and finite amplitude parameter perturbations, the grassland (desert) ecosystem induced by CNOP-P-type climate change was nonlinearly unstable. For the same parameter perturbation amplitude, the response of the grassland (desert) ecosystem to nonlinear climate change was more intense than the response to linear climate change. An abrupt change occurred in the nonlinear conversion of the grassland (desert) ecosystem in the context of the CNOP-P. During this transition, the soil moisture in the root zone and the wilted biomass play crucial roles in the grassland ecosystem. Furthermore, the numerical results reveal that these findings are optimization time- and reference state-independent.

In our study, a theoretical model was applied to assess the response of the grassland ecosystem using the CNOP-P approach. Our study presents a new way to discuss the impact of nonlinear climate change on the grassland ecosystem. However, the model specifically dealt with the stability of the grassland ecosystem of the Inner Mongolia region. Other theoretical models (Klausmeier, 1999; Sherratt and Lord, 2007) may have exhibited nonlinear characteristics using the CNOP approach in other regions. In addition, it would be worthwhile to examine the response using more complex models, including the Lund-Potsdam-Jena (Sitch et al., 2003) model and the Biosphere-Atmosphere Transfer Scheme [BATS, Dickinson et al. (1986); Dickinson et al., 1993]. Mitchell and Csillag (2001)) stated that an increase in precipitation variability decreased stability of the grassland ecosystem, which is corroborated by our work. Previous studies have established the stability of the grassland ecosystem in response to human activity (Mu and Wang, 2007; Sun and Mu, 2009). Taking ecosystem responses to human activity and climate change into account will help lay a sound foundation for ecosystem management.

Acknowledgements. The authors thank the reviewers for their valuable suggestions. This study was supported by National Natural Science Foundation of China (Grant Nos. 40905050, 40805020, 40830955) and the Chinese Academy of Sciences (Grants No. KZCX3-SW-230), LASG Free Exploration Fund, and LASG State Key Laboratory Special Fund.

Table A1. The parameter values in the five-variable ecosystem model.

PA	VA	Explanation
M_c^*	0.1	the characteristic value of the living biomass
M_d^*	0.1	the characteristic value of the wilted biomass
W_s^*	40	the characteristic value of the soil moisture of surface layer
W_r^*	200	the characteristic value of the soil moisture of root zone
α	0.4	the maximum growth rate
β	0.1	the characteristic wilting rate
ϵ_{gx}	1.0	exponential attenuation coefficients about the living biomass in term G
ϵ_{gy_2}	1.0	exponential attenuation coefficients about the soil moisture of root zone in term G
ϵ_{dx}	1.0	exponential attenuation coefficients about the living biomass in term D
ϵ_{dy_2}	1.0	exponential attenuation coefficients about the soil moisture of root zone in term D
γ	0.1	the parameter describing consumption of the living biomass
ϵ_{cx}	1.0	exponential attenuation coefficients about the living biomass in term C_c
β_z	0.1	the characteristic rate of wilted biomass decomposition
ϵ_{dz}	1.0	exponential attenuation coefficients about the wilted biomass in term D_d
e_s^*	1000	the potential evaporation from the bare soil
ϵ_{Esz}	1.0	exponential attenuation coefficients about the wilted biomass in term E_s
ϵ_f	200	the parameter of the fraction of living grass coverage
κ_1	0.4	the parameter describing the vegetation-soil interaction
ϵ_{Esx}	0.7	exponential attenuation coefficients about the living biomass in term E_s
ϵ_{Esy_1}	1.0	exponential attenuation coefficients about the soil moisture of surface layer in term E_s
ϕ_{rs}	0.6	the parameter describing the vegetation-soil interaction
κ_{Er}	1.0	attenuation coefficients about the living biomass in term E_r
ϵ_{Erx}	1.0	exponential attenuation coefficients about the living biomass in term E_r
ϵ_{Ery_2}	1.0	exponential attenuation coefficients about the soil moisture of root zone in term E_r
λ_{rs}	0.015	coefficients about precipitation loss due to surface layer in term R_s
ϵ_{Rsz}	1.0	exponential attenuation coefficients about the wilted biomass in term R_s
κ_{Rs}	0.4	coefficients about the living biomass in term R_s
ϵ_{Rsx}	0.7	exponential attenuation coefficients about the living biomass in term R_s
ϵ_{Rsy_1}	1.0	exponential attenuation coefficients about the soil moisture of surface layer in term R_s
λ_{Rr}	0.015	coefficients about precipitation loss due to surface layer in term R_r
ε_{Rry_2}	1.0	exponential attenuation coefficients about the soil moisture of root zone in term R_r
κ_{Rr}	0.7	coefficients about the living biomass in term R_r
ε_{Rrx}	0.7	exponential attenuation coefficients about the living biomass in term R_s
λ_{QS}	1.0	the characteristic timescale
D_s	100	the thickness of surface layer
D_r	500	the thickness of root zone
α_s	0.85	coefficients about loss due to the surface layer in term P_s^*
α_c	0.05	coefficients about loss due to the living biomass in term P_c^*
ε_c	1.0	exponential attenuation coefficients about the living biomass in term P_c^*

Note: PA and VA denote the parameters and their values. The units of M_c^*, M_d^*, W_s^*, W_r^*, α, e_s^*, D_s and D_r are kg m^{-2}, kg m^{-2}, mm, mm, kg m^{-2} yr^{-1}, mm yr^{-1}, mm and mm.

APPENDIX

The Five-Variable Ecosystem Model

In this section, the details of the five-variable grassland ecosystem model are introduced referring to Zeng et al. (2006) and Sun and Mu (2009). In the right terms, G, D_c, and C_c are the growth, the wilting, and the consumption of the living biomass, respectively. D_d and C_d are decomposition and consumption of the wilted biomass, respectively. P_c, P_s, and P_r are atmospheric precipitation in the vegetation canopy, the surface layer of soil, and the rooting layer, respectively. E_c, E_s and E_r represent evaporation from the vegetation canopy, the surface layer of soil and the rooting layer, respectively. R_c, R_s and R_r correspond to transpiration from the three layers. Q_{sr} is the conductive transport term. According to Zeng et al. (2006), to filter the high frequency variations in M_c and M_d, we assume that the equation $dW_c/dt = P_c(M_c) + E_r(M_c, W_r) - E_c(M_c, W_r) - R_c(M_c)$ is in balance. That is, $P_c(M_c) + E_r(M_c, W_r) - E_c(M_c, W_r) - R_c(M_c) = 0$, and C_d and R_c are zero. Next, the right terms of the model are expressed as follows:

$$G = (1 - e^{-\epsilon_{\rm gx} M_{\rm c}/M_{\rm c}^*})(1 - e^{-\epsilon_{\rm gy_2} W_{\rm r}/W_{\rm r}^*}) ,$$

$$D_{\rm c} = \beta(e^{\epsilon_{\rm dx} M_{\rm c}/M_{\rm c}^*} - 1)(1 - e^{-\epsilon_{\rm dy_2} W_{\rm r}/W_{\rm r}^*})^{-1} ,$$

$$C_{\rm c} = \gamma(1 - e^{-\epsilon_{\rm cx} M_{\rm c}/M_{\rm c}^*}) ,$$

$$D_{\rm d} = \beta_{\rm z}(e^{\epsilon_{\rm dz} M_{\rm d}/M_{\rm d}^*} - 1) ,$$

$$E_{\rm s} = e_{\rm s}^* e^{-\epsilon_{\rm Esz} M_{\rm d}/M_{\rm d}^*}\{e^{-\epsilon_{\rm f} M_{\rm c}/M_{\rm c}^*} + (1 - e^{-\epsilon_{\rm f} M_{\rm c}/M_{\rm c}^*})\times [1 - \kappa_1(1 - e^{-\epsilon_{\rm Esx} M_{\rm c}/M_{\rm c}^*})]\}(1 - e^{-\epsilon_{\rm Esy_1} W_{\rm s}/W_{\rm s}^*}) ,$$

$$E_{\rm r} = e_{\rm s}^* \phi_{\rm rs}(1 - e^{-\epsilon_{\rm f} M_{\rm c}/M_{\rm c}^*})(1 - \kappa_{\rm Er} e^{-\epsilon_{\rm Erx} M_{\rm c}/M_{\rm c}^*})\times (1 - e^{-\epsilon_{\rm Ery_2} W_{\rm r}/W_{\rm r}^*}) ,$$

$$R_{\rm s} = \lambda_{\rm rs} P_{\rm s} e^{-\epsilon_{\rm Rsz} M_{\rm d}/M_{\rm d}^*}\{e^{-\epsilon_{\rm f} M_{\rm c}/M_{\rm c}^*} + (1 - e^{-\epsilon_{\rm f} M_{\rm c}/M_{\rm c}^*})\times [1 - \kappa_{\rm Rs}(1 - e^{-\epsilon_{\rm Rsx} M_{\rm c}/M_{\rm c}^*})]\} \times (e^{\epsilon_{\rm Rsy_1} W_{\rm s}/W_{\rm s}^*} - 1) ,$$

$$R_{\rm r} = \lambda_{\rm Rr} P_{\rm r}(e^{\varepsilon_{\rm Rry_2} W_{\rm r}/W_{\rm r}^*} - 1)[1 - \kappa_{\rm Rr}(1 - e^{-\varepsilon_{\rm Rrx} M_{\rm c}/M_{\rm c}^*})] ,$$

$$Q_{\rm sr} = \lambda_{\rm QS} \frac{D_{\rm s} D_{\rm r}}{D_{\rm s} + D_{\rm r}}\left(\frac{W_{\rm s}}{W_{\rm s}^* D_{\rm s}} - \frac{W_{\rm r}}{W_{\rm r}^* D_{\rm r}}\right) .$$

$P_{\rm c} + P_{\rm s} + P_{\rm r} = P_{\rm rec}$, $P_{\rm c} = \min(P_{\rm c}^*, P_{\rm rec})$, $P_{\rm s} = \min(P_{\rm s}^*, P_{\rm rec} - P_{\rm c})$, $P_{\rm c}^*$ and $P_{\rm s}^*$ are the permissibly upper bounds of $P_{\rm c}$ and $P_{\rm s}$ respectively. Here, the precipitation is assumed to be constant. It is assumed that

$$0 \leqslant P_{\rm c}^* \ll P_{\rm rec} , \quad 0 \leqslant P_{\rm s}^* < P_{\rm rec} - P_{\rm c}^* ,$$

and $P_{\rm c}^*$ increases monotonically with $M_{\rm c}$:

$$P_{\rm c}^* = \alpha_{\rm c} P_{\rm rec}(1 - e^{-\varepsilon_{\rm c} M_{\rm c}/M_{\rm c}^*}) .$$

The expressions of the interception of surface layer and root zone respectively are:

$$P_{\rm s}^* = \alpha_{\rm s}(P_{\rm rec} - P_{\rm c}^*) ,$$

$$P_{\rm r} = (1 - \alpha_{\rm s})(P_{\rm rec} - P_{\rm c}^*) .$$

Let $x = M_{\rm c}/M_{\rm c}^*$, $y_1 = W_{\rm s}/W_{\rm s}^*$, $y_2 = W_{\rm r}/W_{\rm r}^*$, $z = M_{\rm d}/M_{\rm d}^*$ and $t'' = t/t^*$ be the dimensionless variables of the corresponding state variables. The equations of the five-variable ecosystem model related to the living biomass and the wilted biomass are multiplied by $t^*/M_{\rm c}^*$ and $t^*/M_{\rm d}^*$, and the equations related to the soil moisture of surface layer and root zone are respectively multiplied by $(e_{\rm s}^*)^{-1}$. The equations of the five-variable ecosystem model will be nondimensionalized. In our study, we introduce a dimensionless variable

$$\mu = P/e_{\rm s}^* ,$$

where μ is called the moisture index and is one of the important parameters for describing climatic conditions. The parameters of the above expressions are shown in Table A1.

REFERENCES

Barclay, A., P. E. Gill, and J. B. Rosen, 1997: SQP methods and their application to numerical optimal control. Numerical Analysis Report 97-3, Department of Mathematics, University of California, San Diego, La Jolla, CA, 14pp.

Claussen, M, C. Kubatzki, V. Brovkin, A. Ganopolski, P. Hoelzmann, and H. J. Pachur, 1999: Simulation of an Abrupt Change in Saharan Vegetation in the Mid-Holocene. *Geophys. Res. Lett.*, **26**(14), 2037–2040.

Dickinson, R. E., A. Henderson-Sellers, P. J. Kennedy, and M. F. Wilson, 1986: Biosphere-Atmosphere Transfer Scheme (BATS) for the NCAR Community Climate Model. NCAR Technical Note NCAR/TN275+ STR, 69pp.

Dickinson, R. E., A. Henderson-Sellers, and P. J. Kennedy, 1993: Biosphere-Atmosphere Transfer Scheme (BATS) version 1e as coupled to the NCAR Community Climate Model. NCAR Technical Note NCAR/TN-387+STR, 72pp.

Duan, W. S., M. Mu, and B. Wang, 2004: Conditional nonlinear optimal perturbation as the optimal precursors for El Niño-Southern Oscillation events. *J. Geophys. Res.*, **109**, D23105, doi: 10.1029/2004JD004756.

Duan, W. S., and M. Mu, 2006: Investigating decadal variability of El Niño Southern Oscillation asymmetry by conditional nonlinear optimal perturbation. *J. Geophys. Res.*, **111**, C07015, doi: 10.1029/2005JC003458.

Gao, X. J., Y. Luo, W. T. Lin, Z. C. Zhao, and G. Filippo, 2003: Simulation of Effects of Land Use Change on Climate in China by a Regional Climate Model. *Adv. Atmos. Sci.*, **20**(4), 583–592.

Hallgren, W. S., and A. J. Pitman, 2000: The uncertainty in simulations by a global biome model (BIOME3) to alternative parameter values. *Global Change Biology*, **6**(5), 483–495.

Jia, B. R., G. S. Zhou, F. Y. Wang, Y. H. Wang, and E. S. Weng, 2007: Effects of Grazing on Soil Respiration of Leymus Chinensis Steppe. *Climatic Change*, **82**, 211–223.

Klausmeier, C. A., 1999: Regular and irregular patterns in semiarid vegetation. *Science*, **284**(5421), 1826–1828.

Liu, Z., M. Notaro, J. Kutzbach, and N. Liu, 2006a: Assessing Global Vegetation-Climate Feedbacks from Observations. *J. Climate*, **19**, 787–814.

Liu, Z. Y., Y. Wang, R. Gallimore, M. Notaro, and I. C. Prentice, 2006b: On the cause of abrupt vegetation collapse in North Africa during the Holocene: Climate variability vs. vegetation feedback. *Geophys. Res. Lett.*, **33**, L22709, doi: 10.1029/2006GL028062.

Ma, Z. G., and C. Fu, 2001: Trend of surface humid index in the arid area of northern China. *Acta Meteorologica Sinica*, **59**(6), 737–746. (in Chinese)

Mitchell, S. W., and F. Csillag, 2001: Assessing the stability and uncertainty of predicted vegetation growth under climatic variability: Northern mixed grass prairie. *Ecological Modelling*, **139**(2–3), 101–121.

Mu, M., and W. S. Duan, 2003: A new approach to studying ENSO predictability: Conditional nonlinear optimal perturbation. *Chinese Science Bulletin*, **48**, 1045–1047.

Mu, M., and B. Wang, 2007: Nonlinear instability and sensitivity of a theoretical grassland ecosystem to finite-amplitude perturbations. *Nonlinear Processes in Geophysics*, **14**, 409–423.

Mu, M., and Z. N. Jiang, 2008: A new approach to the generation of initial perturbations for ensemble prediction: Conditional nonlinear optimal perturbation. *Chinese Science Bulletin*, **53**(13), 2062–2068.

Mu, M., W. S. Duan, and B. Wang, 2003: Conditional nonlinear optimal perturbation and its applications. *Nonlinear Processes in Geophysics*, **10**, 493–501.

Mu, M., L. Sun, and H. A. Dijikstra, 2004: The sensitivity and stability of the ocean's thermohaline circulation to finite amplitude perturbations. *Journal of Physical Oceanography*, **34**, 2305–2315.

Mu, M., W. S. Duan, and B. Wang, 2007a: Season-dependent dynamics of nonlinear optimal error growth and El Nino- Southern Oscillation predictability in a theoretical model. *J. Geophys. Res.*, **112**, D10113, doi: 10.1029/2005JD006981.

Mu, M., H. L. Wang, and F. F. Zhou, 2007b: A Preliminary application of conditional nonlinear optimal perturbation to adaptive observation. *Chinese J. Atmos. Sci.*, **31**(6), 1102–1112. (in Chinese)

Mu, M., W. Duan, Q. Wang, and R. Zhang, 2010: An extension of conditional nonlinear optimal perturbation approach and its applications, *Nonlinear Processes in Geophysics*, **17**, 211–220, doi: 10.5194/npg-17-211-2010.

Ni, J., 2004: Estimating grassland net primary productivity from field biomass measurements in temperate northern China. *Plant Ecology*, **174**(2), 217–234.

Notaro, M., Z. Liu, and J. W. Williams, 2006: Observed Vegetation-Climate Feedbacks in the United States. *J. Climate*, **19**, 763–786.

Piao, S. L., J. Y. Fang, L. Zhou, K. Tan, and S. Tao, 2007: Changes in biomass carbon stocks in China's grasslands between 1982 and 1999. *Global Biogeochemical Cycles*, **21**, GB2002, doi: 10.1029/2005GB002634.

Rosero, E., Z. L. Yang, T. Wagener, L. E. Gulden, S. Yatheendradas, and G.Y. Niu, 2010: Quantifying parameter sensitivity, interaction, and transferability in hydrologically enhanced versions of the Noah land surface model over transition zones during the warm season, *J. Geophys. Res.*, **115**, D03106, doi: 10.1029/2009JD012035.

Sherratt, J. A., and G. J. Lord, 2007: Nonlinear dynamics and pattern bifurcation in a model for vegetation stripes in semi-arid environments. *Theoretical Population Biology*, **71**, 1–11.

Sitch, S., and Coauthors, 2003: Evaluation of ecosystem dynamics, plant geography and terrestrial carbon cycling in the LPJ Dynamic Vegetation Model. *Global Change Biology*, **9**, 161–185.

Sun, L., M. Mu, D. J. Sun, and X. Y. Yin, 2005: Passive mechanism of decadal variation of thermohaline circulation. *J. Geophys. Res.*, **110**, C07025, doi: 10.1029/2005JC002897.

Sun, G. D., and M. Mu, 2009: Nonlinear feature of the abrupt transitions between multiple equilibria states of an ecosystem model. *Adv. Atmos. Sci.*, **26**(2), 293–304, doi: 10.1007/s00376-009-0293-8.

Woodward, F. I., 1987: *Climate and Plant Distribution*. Cambridge University Press, 174pp.

Woodward, F. I., M. R. Lomas, and C. K. Kelly, 2004: Global climate and the distribution of plant biomes. *Philos. Trans. Roy. Soc. London*, **359B**, 1465–1476.

Xue, Y. K., and J. Shukla, 1993: The influence of land surface properties on Sahel climate. Part I: desertification. *J. Climate*, **6**, 2232–2245.

Xue, Y., 1996: The Impact of Desertification in the Mongolian and the Inner Mongolian Grassland on the Regional Climate. *J. Climate*, **9**, 2173–2189.

Zeng, N., and J. D. Neelin, 2000: The role of vegetation-climate interaction and interannual variability in shaping the African Savanna. *J. Climate*, **13**, 2665–2670.

Zeng, N., K. Hales, and J. D. Neelin, 2002: Nonlinear dynamics in a coupled vegetation-atmosphere system and implications for desert-forest gradient. *J. Climate*, **15**, 3474–3487.

Zeng, X. D., S. S. P. Shen, X. B. Zeng, and R. E. Dickinson, 2004: Multiple equilibrium states and the abrupt transitions in a dynamical system of soil water interacting with vegetation. *Geophys. Res. Lett.*, **31**, 5501, doi: 10.1029/2003GL018910.

Zeng, X. D., X. B. Zeng, S. S. P. Shen, R. E. Dickinson, and Q. C. Zeng, 2005: Vegetation-soil water interaction within a dynamical ecosystem model of grassland in semi-arid areas. *Tellus*, **57B**, 189–202.

Zeng, X. D., A. H. Wang, Q. C. Zeng, R. E. Dickinson, X. B. Zeng, and S. S. P. Shen, 2006: Intermediately complex models for the hydrological interactions in the atmosphere-vegetation-soil system. *Adv. Atmos. Sci.*, **23**(1), 127–140.